



Published in final edited form as:

Circulation. 2015 March 31; 131(13): 1202–1213. doi:10.1161/CIRCULATIONAHA.114.012669.

## Knockout of *Adamts7*, A Novel CAD Locus in Humans, Reduces Atherosclerosis in Mice

Robert C. Bauer, PhD<sup>1,2</sup>, Junichiro Tohyama, MD, PhD<sup>1,2</sup>, Jian Cui, MD<sup>1,3</sup>, Lan Cheng, MS<sup>1,3</sup>, Jifu Yang, MD<sup>1,3</sup>, Xuan Zhang, PhD<sup>1,3</sup>, Kristy Ou, BS<sup>1,3</sup>, Georgios K. Paschos, PhD<sup>1,4</sup>, X. Long Zheng, MD, PhD<sup>5</sup>, Michael S. Parmacek, MD<sup>1,3</sup>, Daniel J. Rader, MD<sup>#1,2,3,4</sup>, and Muredach P. Reilly, MBBCH, MSCE<sup>#1,3</sup>

<sup>1</sup>The Perelman School of Medicine at the University of Pennsylvania, Philadelphia, PA

<sup>2</sup>Division of Translational Medicine and Human Genetics, Philadelphia, PA

<sup>3</sup>The Cardiovascular Institute, Philadelphia, PA

<sup>4</sup>The Institute of Translational Medicine and Therapeutics, Philadelphia, PA

<sup>5</sup>The Children's Hospital of Philadelphia Department of Pathology and Laboratory Medicine, Philadelphia, PA

# These authors contributed equally to this work.

### Abstract

**Background**—Genome-wide association studies (GWAS) have established *ADAMTS7* as a locus for coronary artery disease (CAD) in humans. Yet, these studies fail to provide directionality for the association between *ADAMTS7* and CAD. Previous reports have implicated *ADAMTS7* in the regulation of vascular smooth muscle cell (VSMC) migration, but a role and direction of impact for this gene in atherogenesis has not been shown in relevant model systems.

**Methods and Results**—We bred an *Adamts7* whole body knockout (KO) mouse onto both the *Ldlr* and *ApoE* KO hyperlipidemic mouse models. *Adamts7*<sup>-/-</sup>/*Ldlr*<sup>-/-</sup> and *Adamts7*<sup>-/-</sup>/*ApoE*<sup>-/-</sup> mice displayed significant reductions in lesion formation in aortas and aortic roots as compared to controls. *Adamts7* KO mice also showed reduced neointimal formation after femoral wire injury. *Adamts7* expression was induced in response to injury and hyperlipidemia but was absent at later timepoints, and primary *Adamts7* KO VSMCs showed reduced migration in the setting of TNF $\alpha$  stimulation. *ADAMTS7* localized to cells positive for SMC markers in human CAD lesions, and sub-cellular localization studies in cultured VSMCs placed *ADAMTS7* at the cytoplasm and cell membrane, where it co-localized with markers of podosomes.

**Conclusions**—These data represent the first *in vivo* experimental validation of the association of *Adamts7* with atherogenesis, likely through modulation of vascular cell migration and matrix in atherosclerotic lesions. These results demonstrate that *Adamts7* is proatherogenic, lending

**Correspondence:** Muredach P. Reilly, MBBCH, MSCE The Perelman School of Medicine at the University of Pennsylvania 11-136 Translational Research Center, 3400 Civic Center Blvd., Philadelphia PA 19104-6160 Phone: 215-573-1214 Fax: 215-573-9004 muredach@mail.med.upenn.edu.

**Disclosures:** None.

directionality to the original genetic association and supporting the concept that pharmacological inhibition of ADAMTS7 should be atheroprotective in humans, making it an attractive target for novel therapeutic interventions.

### Keywords

ADAMTS7; metalloproteinases; atherosclerosis; coronary artery disease; genome wide association study; knockout mouse

---

## INTRODUCTION

Coronary artery disease (CAD) is a heritable disease and a leading cause of death and morbidity<sup>1</sup>. Recent large-scale genome-wide association studies (GWAS) have discovered and replicated over forty loci for CAD and myocardial infarction (MI). One of these loci on chromosome (chr) 15 contains the gene *A* disintegrin and metalloproteinase with thrombospondin motifs-7 (*ADAMTS7*), and was initially identified by our group through GWAS of angiographic CAD<sup>2</sup>. This finding has since been replicated multiple times for both CAD and MI in further meta-analyses, suggesting that *ADAMTS7* is a novel regulator of atherogenesis in humans<sup>3-5</sup>. To date, however, the lack of human expression quantitative trait loci (eQTL) data in relevant tissues creates uncertainty about whether *ADAMTS7* is the causal gene at the locus and prevents elucidation of the directionality between the actions of *ADAMTS7* and disease pathogenesis.

*ADAMTS7* is a member of the ADAMTS family of secreted zinc metalloproteases with characteristic protein domain composition including at least one thrombospondin type I repeat (TSPI)<sup>6,7</sup>. These proteins have highly homologous N-terminal protein domain structure and organization, but the C-terminal halves of these proteins vary significantly which is believed to confer substrate specificity to the proteins<sup>8,9</sup>. Previous research on *ADAMTS7* has mainly centered on its role in bone and cartilage growth because cartilage oligomeric matrix protein (COMP) has been identified as a substrate<sup>10</sup>. *ADAMTS7* can regulate endochondral bone formation through interactions with COMP<sup>11</sup>, but COMP is also expressed in VSMC and vasculature<sup>12</sup>. Additional studies with viral-mediated overexpression and knock-down *in vivo* and *in vitro* suggests that *ADAMTS7* might modulate VSMC phenotype switching and migration<sup>13</sup>.

Here we present the first report of an *Adamts7* knockout (*Adamts7*<sup>-/-</sup>) mouse, and demonstrate that *Adamts7* deficiency in both the *Ldlr*<sup>-/-</sup> and *ApoE*<sup>-/-</sup> hyperlipidemic mouse models markedly attenuates formation of atherosclerotic lesions; furthermore, wire-injury experiments in the *Adamts7*<sup>-/-</sup> mouse show reduced neointima formation. We demonstrate that *Adamts7* gene expression is induced transiently in the mouse vasculature in response to stress, both in the wire injury model and in the atherosclerosis experiments, that TNF $\alpha$  induces *Adamts7* expression in primary VSMCs, and that VSMC of *Adamts7*<sup>-/-</sup> mice show reduced TNF $\alpha$ -induced migration. Finally, immunostaining in human diseased coronary arteries reveals colocalization of ADAMTS7 with cells positive for VSMC markers, and immunofluorescence in human aortic smooth muscle cells (hAoSMCs) shows subcellular localization with leading edges of migrating VSMCs.

## METHODS

Full expanded methods are available in the Supplemental Material, including methods for Generation of *Adamts7* mouse strains, Plasma Lipid Measurements, X-gal Staining, Vascular Injury Studies, Primary Aortic VSMC studies, Aortic SMC Immunofluorescence, and *Immunohistochemistry*.

### Atherosclerosis Studies

*Adamts7*<sup>-/-</sup> mice were crossed onto the *Ldlr* and *Apoe* hyperlipidemic KO mouse backgrounds, and single knockout (KO) (*Ldlr* or *Apoe* alone) and double KO (dKO) mice were obtained. Experimental dKO mice, 8-12 weeks of age, and control littermates were fed western diet (D12079Bi, Research Diets) for 16 weeks (*Adamts7/Ldlr*) or 10 weeks (*Adamts7/Apoe*) and then mice were euthanized. Aortas were collected from the base of ascending aorta to the iliac bifurcation for en face lesion measurement, while aortic roots and brachiocephalic arteries (BCAs) were either X-gal stained as described above, or paraffin embedded and used for lesion area quantification and immunohistochemistry (IHC).

For atherosclerosis lesion quantification, whole aortas were stained with oil red O as previously described<sup>14</sup>, and then positively staining lesion area was measured and data reported as a percentage of entire aortic area. For aortic roots, lesion area was measured on hematoxylin and eosin (H/E) stained sections from paraffin embedded hearts. We quantified lesion area in 5 serial sections (80um between sections). For selection of the 5 sections, we defined a “zero point” which is the first section which captures all 3 leaflets of the aortic valve moving from the aortic arch towards the ventricles. Then the two serial sections proximal (+1 and +2) and distal (-1 and -2) to the zero point were quantified. For each mouse, the data was represented as either the average lesion area (average area across the 5 points) or as the area under the curve (AUC) produced by integration of the total areas across all 5 sections (i.e., the “integrated AUC” of root lesions).

### Statistical Analysis

Data are presented as mean and all error bars represent standard error. Statistical significance was tested using unpaired Students t-tests and a *p*-value of 0.05 was considered significant. For atherosclerosis studies, unpaired t-tests were used to compare percent lesion area of aorta (en face) or actual lesion area (aortic roots) of *Adamts7*<sup>-/-</sup> animals to control *Adamts7*<sup>+/+</sup> animals for each gender separately. For vascular injury studies, unpaired t-tests were used to compare neointimal area, neointima-media ratio, and percent stenosis of *Adamts7*<sup>-/-</sup> animals to control *Adamts7*<sup>+/+</sup>. In VSMC migration assays, unpaired t-tests were used to compare the percentage of the original area remaining in VSMCs of *Adamts7*<sup>-/-</sup> vs. *Adamts7*<sup>+/+</sup> control animals. For qPCR studies, results from untreated *Adamts7*<sup>+/+</sup> cells/tissue were set to 1 and all other groups compared to that group via unpaired t-test.

## RESULTS

### Characterization of *Adamts7* expression in WT and KO mice

We examined *Adamts7* mRNA expression in a variety of murine tissues harvested from C57BL/6 WT females. *Adamts7* expression varied greatly between tissues (Figure 1A) with the highest levels in heart, brain, lung, intestine and adrenal gland. By contrast, low, but detectable levels were observed in liver, spleen, kidney, brown fat, thyroid and skeletal muscle. We commissioned the generation of an *Adamts7* knockout mouse (*Adamts7*<sup>-/-</sup>) in which the gene was ablated using a gene trap strategy with  $\beta$ -galactosidase gene (*lacZ*) insertion into intron 4 of the *Adamts7* locus (Figure 1B). By design, splicing from exon 4 to the gene trap cassette results in a severely truncated protein containing only the signal peptide, prodomain, and a small portion of the metalloprotease domain. The trapping cassette contains a *LacZ* reporter gene allowing for X-gal staining as readout of active *Adamts7* expression. *Adamts7* gene knock-out was verified by real-time qPCR using two probe sets, one that spans the exon 5-6 junction and one that spans the exon 23-24 junction (Figure 1C). *Adamts7*<sup>-/-</sup> animals exhibited >95% reduction of the message in heart and lung (Figure 1C). X-Gal staining of multiple tissues from *Adamts7*<sup>-/-</sup> mice was consistent with the mRNA expression data from C57BL/6 mice and confirmed that the reporter was working. High levels of  $\beta$ -galactosidase activity were observed in the heart and pulmonary vasculature but not other tissues such as the liver and spleen (Figure 1D). IHC analysis for markers of cardiomyocytes ( $\alpha$ -Actinin), endothelial cells (PECAM-1), and epithelial cells (E-Cadherin) localized the positive X-gal staining, and thus *Adamts7* expression, to the myocardium of the heart and the tunica media of the pulmonary vasculature (Supplemental Figure 1). *Adamts7*<sup>-/-</sup> mice display no outward phenotypes, reproduce normally and appear healthy under chow-fed conditions.

### *Adamts7* KO decreases atherosclerosis in hyperlipidemic mouse models

Atherosclerosis was quantified in *Adamts7/Ldlr* and *Adamts7/Apoe* double KO (dKO) mice and control littermates. Mice were fed western diet for 16 weeks (*Ldlr*) or 10 weeks (*Apoe*). Aortas and aortic roots were harvested for lesion area quantification while root and BCA sections were used for lesion characterization by IHC. On western diet, no differences in plasma lipid levels were observed between experimental groups (Supplemental Table 1).

*Adamts7/Ldlr* dKO males (N=31) and females (N=34) displayed significant reductions in aortic lesion area as measured by en face (37%,  $p=0.001$  and 52%,  $p<0.0001$  respectively) (Figure 2A,B). Similarly, aortic roots from *Adamts7/Ldlr* dKO males and females showed decreased lesion area (32%,  $p=0.001$  and 25%,  $p<0.0001$  respectively) compared to control *Ldlr*<sup>-/-</sup> male (N=21) and female (N=28) littermates (Figure 2C,D; Supplemental Figure 2A-D).

Marked reductions in atherosclerosis were seen also on the *Apoe*<sup>-/-</sup> background; *Adamts7/Apoe* dKO males (N=16) and females (N=13) displayed significantly reduced lesion formation by en face (62%,  $p<0.0001$  and 54%,  $p<0.0001$  respectively) (Figure 3A,B), and similar pattern in aortic roots (18%,  $p=0.07$  and 22%,  $p=0.04$  respectively) compared to

control *ApoE*<sup>-/-</sup> males (N=9) and females (N=10) (Figure 3C,D; Supplemental Figure 2E-H).

We characterized the cellular and collagen composition of aortic root and BCA lesions from the *Adamts7/Ldlr* dKO animals and their control *Ldlr*<sup>-/-</sup> littermates (N=8/group, average of 3-serial sections/animal) by IHC or Masson's trichrome staining of lesions with subsequent quantification. No significant difference in SMC content (SM22-positive signal) or intensity of contractile marker staining (e.g., SM-MyHC) was observed in BCA lesions but trends toward reduced macrophage and increased collagen content were observed in BCAs (Figure 4E-H). A similar pattern of increased collagen in aortic roots of atherosclerotic mice was observed (Supplemental Figure 3)

### **Adamts7 deficiency reduces the neointimal response to vascular injury and TNF $\alpha$ -stimulated-migration of smooth muscle cells**

Previous reports have implicated ADAMTS7 in smooth muscle cell phenotype modulation in response to vascular injury<sup>15</sup>. To examine the role of Adamts7 in the response to vascular injury, we performed femoral artery wire-injury and sham surgeries on *Adamts7*<sup>-/-</sup> and WT littermates. Compared to WT littermates at 28-days post injury, *Adamts7* null animals displayed a 64% reduction ( $p=0.05$ ) in neointima formation (Figure 5A,B), a 47% reduction in intima-to-media ratio (Figure 5C), and a 61% decrease in percent stenosis ( $p=0.003$ ) (Figure 5D). Coincident with this reduction in neointima, expression of contractile markers within neointima, including SM-MyHC, SM- $\alpha$ -actin and SM22 $\alpha$  was significantly greater in *Adamts7*<sup>-/-</sup> mice following vascular injury compared to control mice (Supplemental Figure 4). Thus, following acute mechanical vascular injury, ablation of the *Adamts7* gene reduced neointimal formation and appeared to maintain VSMC phenotype.

In light of vascular injury findings, we tested whether primary aortic SMCs from *Adamts7*<sup>-/-</sup> mice had reduced migration compared to those from control WT littermates. In initial studies, WT and KO VSMCs plated on collagen I, fibronectin, laminin, or uncoated plates displayed no differences in migratory ability. In prior studies of rat primary VSMCs, TNF $\alpha$  induced *Adamts7* expression<sup>13</sup>, so we examined TNF $\alpha$  effects in WT VSMC and found a similar upregulation (~6-fold,  $p=0.0007$ ) of *Adamts7* (Figure 5E). Migration studies performed following 24-hours of TNF $\alpha$  treatment revealed a reduction in migration of TNF $\alpha$ -stimulated *Adamts7*<sup>-/-</sup> VSMCs compared to WT cells in dishes coated with collagen or laminin (Figure 5F,G), while unstimulated cells showed no difference (Supplemental Figure 5). This supports the concept that *in vitro*, protective VSMC phenotypes in *Adamts7*<sup>-/-</sup> are revealed in the setting of inflammatory stress, consistent with the observed vascular protection during *in vivo* physical and hyperlipidemic vascular insults.

### **Adamts7 expression is temporal and transient during vascular injury and in atherosclerosis**

Our data suggests that Adamts7 modulates VSMC phenotype and migration during inflammatory stress and mechanical injury and that *Adamts7* deficiency markedly reduces atherosclerotic lesions in hyperlipidemic mice. Yet the atherosclerosis data did not yield clear differences in relative matrix or SMC composition of lesions at the time of sacrifice

(16-weeks and 10-weeks western diet feeding in *Ldlr*<sup>-/-</sup> and *ApoE*<sup>-/-</sup> models, respectively). Thus, we posited that murine *Adamts7* might function predominantly in early lesion formation and that the imprint of *Adamts7* deficiency is less visible on specific morphologies in more mature murine lesions. The  $\beta$ -galactosidase reporter in the exon-trapping cassette of the *Adamts7*<sup>-/-</sup> mouse (Figure 1B) permits X-gal staining in harvested tissues allowing identification of cells that actively transcribe the *Adamts7* gene in animals carrying a KO allele. In light of the lack of working antibodies towards mouse *Adamts7*, we used this approach to examine the time course of vascular expression of *Adamts7* in our vascular wire-injury model as well as in atherosclerosis models.

First, we studied various time-points after femoral wire injury (N=4/timepoint). At day-1 post-injury (Figure 6A) and day-28 post-injury (time of harvest, data not shown), we saw no evidence of X-gal staining. However, at day-7 post-injury (Figure 6B) blue staining indicative of  $\beta$ -galactosidase expression was apparent in injured vessels, predominantly localized to the media and adventitia, and this staining was almost completely absent at day-14 (Figure 6C). When considered in context of reduction in day-28 lesions following injury in *Adamts7*<sup>-/-</sup> mice, this suggests that *Adamts7* expression is induced early and transiently in response to the acute injury and impacts the day-28 remodeling through its actions during the early pathophysiological response. Thus, the effects of *Adamts7* deletion during injury may be confined to the early phase when VSMC migration plays a critical role<sup>16</sup>.

In this context, we analyzed X-gal staining patterns in BCA and aortic roots from *Adamts7*<sup>-/-</sup>;*ApoE*<sup>-/-</sup> mice fed western diet for varying lengths of time (N=3/timepoint). BCAs from mice fed western diet for 1 week showed no atherosclerotic lesion formation and no positive X-gal staining (Figure 6D). At 4 weeks on western diet, however, a subset of *Adamts7*<sup>-/-</sup>;*ApoE*<sup>-/-</sup> mice had developed lesions in the BCA, and these displayed strong positive X-gal staining in the both media and lesion neointima (Figure 6E). IHC analysis of these lesions showed overlap with cells positive for SM- $\alpha$ -actin but not SM22 (Supplemental Figure 6). In support of a transient induction of *Adamts7* during development of atherosclerosis, X-gal staining was not observed in BCA lesions at later time-points (e.g. 10-weeks) even though mature atherosclerotic plaques were present (Figure 6F). A similar pattern was observed in aortic roots of these mice; the only positive X-gal staining was observed in roots from mice fed western diet for 4-weeks (data not shown). X-gal staining of cultured primary VSMCs of *Adamts7*<sup>-/-</sup> mice revealed modest positive staining under resting conditions, but this X-gal staining was markedly increased following treatment with TNF $\alpha$  (Figure 6G). These observations suggest that *Adamts7* is induced transiently and expressed only during earlier stages of atherogenesis in mouse, likely via inflammatory (e.g., TNF $\alpha$ ) and hyperlipidemic triggers. This is consistent with its induction in the early phase of femoral artery injury and suggests that *Adamts7* may be active at early phases of both mechanical vascular injury and western diet/hyperlipidemia-induced vascular stress and atherosclerosis.



## ADAMTS7 is expressed in human atherosclerosis and localizes to the migrating edge of VSMC

Our rodent data suggest a role for *Adamts7* in promoting VSMC phenotypic transition and migration during arterial injury and hyperlipidemic atherogenic stress. In order to place these rodent observations in a human context, we obtained sections of diseased human coronary arteries (N=12) and performed immunohistochemical studies (Figure 7, Supplemental Figure 7, Supplemental Figure 8). ADAMTS7 consistently colocalized in the vascular media with VSMC markers SM22 and SM- $\alpha$ -actin in all lesions examined (Figure 7A-D). In fibrotic atherosclerotic lesions, ADAMTS7 also colocalized with SM22 positive signal in the neointimal region of the lesion (Figure 7B). Interestingly, in more advanced lesions, SM22 and SM- $\alpha$ -actin consistently stained the fibrous cap but limited ADAMTS7 staining was observed in those regions (Figure 7B, C). Conversely, in these advanced lesions ADAMTS7 staining was observed in the lesion neointima in regions sometimes negative for VSMC markers (Figure 7B, C). By contrast, ADAMTS7 staining did not colocalize with the macrophage marker CD68 in any lesions examined (e.g., Figure 7E). These data show that ADAMTS7 is expressed in human arteries and lesions in medial VSMCs, and suggest that ADAMTS7 stains neointimal cell populations, only a subset of which express classic VSMC markers.

To determine the sub-cellular localization of ADAMTS7 in human VSMCs, we also performed immunofluorescence in primary hAoSMCs. Anti-ADAMTS7 staining demonstrated abundant protein expression in cytoplasmic granules as well as at the cell membrane (Figure 8A). ADAMTS7 was also found at the leading edge of cells and co-localized with cytoskeletal filaments as well as Na<sup>+</sup>/K<sup>+</sup> ATPase, a cell surface expressed protein (Figure 8B, C). Further, ADAMTS7 co-localized at the cell membrane with cortactin (Figure 8D), a marker of focal adhesions and podosomal complexes that orchestrate VSMC migration through vascular matrix<sup>17</sup>.

## DISCUSSION

Through GWAS, we identified *ADAMTS7* as a novel locus for CAD in humans<sup>2</sup>. The association with this chr15 locus has been reproduced in independent large GWAS meta-analyses<sup>3-5</sup>. The *ADAMTS7* locus, however, has no relationship to traditional risk factors, the direction of its action in atherosclerosis is unknown, and precise mechanisms of action in atherosclerosis remain to be determined; indeed it has remained uncertain as to whether ADAMTS7 is definitely the causal gene at the locus. Here, we present the first report of *Adamts7*<sup>-/-</sup> mice and show that *Adamts7* deficiency causes marked protection from western diet-induced atherosclerosis in multiple hyperlipidemic mouse models, reduced neointimal formation following arterial injury, and decreased VSMC migration *in vitro*. These data not only strongly implicate ADAMTS7 as the causal gene at this human CAD locus, but also provide evidence for a pro-atherogenic role of the gene *in vivo* and conversely an anti-atherogenic effect of its genetic inhibition. Overall, our findings in two well-validated rodent model systems suggest that ADAMTS7 promotes atherosclerosis and that targeting its function could be a novel therapeutic strategy for atherosclerosis, CAD and MI in humans.

Recent GWAS have identified over 40 loci for CAD and MI. Unlike *ADAMTS7*, few novel loci have the combination of a clear candidate at the locus and plausible biology for the candidate gene. We discovered *ADAMTS7* as a locus for coronary atherosclerosis using angiographic CAD as the outcome, and subsequent studies have shown that *ADAMTS7* also relates to MI. However, its association is most robust for angiographic CAD, a marker of coronary atherosclerotic burden, suggesting that *ADAMTS7* is likely to relate to clinical events through the development and progression of atherosclerosis. Our current findings in mice are consistent with such an action in the clinical setting.

The family of ADAMTS proteases degrades ECM and has grown to 19 members. ADAMTS family members are associated with vascular diseases including thrombotic thrombocytopenic purpura (TTP)<sup>18</sup>, Weill-Marchesani syndrome<sup>19</sup> and atherosclerosis<sup>20</sup>. Like all ADAMTS proteins, *ADAMTS7* includes a signal peptide, a pro-domain, a catalytic domain, a disintegrin-like domain, a central thrombospondin type I (TS)-like repeat, a cysteine-rich domain, a spacer region, and seven C-terminal TS repeats<sup>15</sup>. Unlike other metalloproteinases, ADAMTSs demonstrate narrow substrate specificity due to their C-terminal exosites. *ADAMTS7* has been implicated in bone development and in inflammatory arthritis through degradation of COMP, a pentameric glycoprotein involved in inherited human chondrodysplasias<sup>10</sup>. Previously published data suggest that the *ADAMTS7*-COMP interaction may extend to the vasculature. VSMC phenotypic switching and matrix remodeling play important roles in vascular disease and contribute to the development and progression of atherosclerosis. Studies in rat suggest that COMP may maintain VSMCs in a contractile phenotype<sup>21</sup>. Adenoviral over-expression of *ADAMTS7* increased COMP cleavage and neointima in injured arteries while over-expression of COMP blocked *ADAMTS7* effects<sup>13</sup>. Whether acute effects using transient over-expression extend to vascular pathophysiology and atherosclerosis during germline modulation had not been studied.

Most domains in human and mouse *Adamts7* are highly conserved rendering the mouse as a useful model for actions in human disease. We obtained whole-body KO mice and bred them onto both the *Ldlr*<sup>-/-</sup> and *ApoE*<sup>-/-</sup> KO hyperlipidemic mouse models and performed atherosclerosis studies in both males and females of each strain. Loss of *Adamts7* clearly and significantly reduced atherosclerotic burden in the aortas and aortic roots of these mice in both sexes and both strains. Femoral artery wire injury is an established model in mouse for studying VSMC phenotype transitions and matrix remodeling during vascular injuries of relevance to clinical vascular pathophysiology, e.g., restenosis during coronary angioplasty and stent implantation. At 28 days following femoral injury or sham surgery, *Adamts7*<sup>-/-</sup> mice had reduced neointima formation and intima-to-media ratio compared to WT. Primary aortic VSMCs from *Adamts7*<sup>-/-</sup> mice displayed decreased migration on collagen and laminin coated plates, but only in the setting of TNF $\alpha$  stimulation. TNF $\alpha$ , a pro-inflammatory cytokine, and more broadly activation of innate immune pro-inflammatory signals have been implicated in atherosclerosis in both rodent hyperlipidemic models<sup>22</sup> and human studies<sup>23</sup>, and also modulate VSMC migration<sup>24</sup>. It is plausible that *ADAMTS7* plays a key role in mediating VSMC responses to inflammatory stresses in atherosclerosis and facilitates VSMC phenotype transition and localized matrix remodeling.



We observed a lack of *Adamts7* expression in mouse aortas under resting conditions. In combination with our data in mouse atherosclerosis and femoral injury, this suggests, at least in these mouse models, that induction of *Adamts7* may be important in VSMC phenotype transition during injury response and development of atherosclerosis but not in murine vascular homeostasis. The lack of any vascular developmental defects in germline *Adamts7* deletion also supports this concept. X-gal staining of mouse vasculature at various time-points after femoral wire injury or western diet feeding confirms that *Adamts7* vascular expression is transient and temporal, peaking early after both mechanical and hyperlipidemic vascular insults. Stimulation of primary VSMCs with TNF $\alpha$  also dramatically increased positive X-gal staining of these cells, suggesting that TNF $\alpha$  (and other pro-inflammatory cytokines) may play a key role in *Adamts7* induction in response to injury.

Understanding the relationship between CAD risk alleles in the *ADAMTS7* genomic region and expression levels of *ADAMTS7* in disease relevant cells could facilitate translation of our rodent findings into human therapeutics. Interestingly, in available eQTL datasets with large sample sizes (e.g., LCL eQTL from the MuTHER study, N=850)<sup>25</sup>, the lead SNPs from the PennCath (rs1994016), CARDIoGRAM (rs3825807), and C4D (rs4380028) GWAS studies display a significant association with *ADAMTS7* expression (eQTL  $p=0.0011$ ,  $0.00097$ , and  $0.0028$  respectively)<sup>25</sup> matching the directionality and causality of our *in vivo* data, i.e., the CAD risk alleles are associated with higher *ADAMTS7* expression. However, currently there are no large eQTL or genomic allelic imbalance data that provide adequate power to determine eQTL directionality in the most pertinent human cells and vascular tissues (i.e., coronary lesions, coronary or aortic SMCs) to more definitely support that *ADAMTS7* functions to promote human atherosclerosis and CAD. Work by our group and consortia such as GTEx will soon produce datasets from a large enough sample pool of human vasculature to address this question. Currently though, our rodent studies provide the first data in established atherosclerosis models that suggests *Adamts7* is proatherogenic *in vivo*. These rodent data are also in broad agreement with a recent report suggesting that a CAD promoting coding variant in humans is associated with reduced *ADAMTS7* protein secretion and function<sup>26</sup>.

Our data strongly suggests that in mouse models of atherosclerosis and vascular injury, *Adamts7* plays a key role in the regulation of VSMC phenotype switching and the development of atherosclerosis. But how the transient and stress-dependent vascular expression pattern of *Adamts7* in mouse relates to what occurs in human disease is uncertain. In an attempt to explore this question, we isolated human coronary arteries and performed IHC for *ADAMTS7* in diseased artery sections. In contrast to mouse aortas, *ADAMTS7* expression was not apparently transient and identified in the media of a wide range of stages and types of human atherosclerosis. In further contrast to mouse, *ADAMTS7* protein was expressed in advanced human lesions in both media and the neointima, predominantly, but not exclusively, colocalizing with cells expressing SMC markers. This may be relevant for clinical and therapeutic translation. Whereas in rodents, it may be necessary to block *Adamts7* function early in the disease process to produce an anti-atherosclerotic effect (ongoing studies), the expression of *ADAMTS7* in advanced

atherosclerotic lesions as well as early lesions suggest that therapeutic inhibition of ADAMTS7 even in established and advanced disease might translate to clinical benefit. Such questions require additional rodent and human experiments and trials.

Finally, we examined ADAMTS7 protein expression in hAoSMCs and found its immunofluorescent localization to both the cytoplasm and cell membrane with specific co-localization to cytoskeletal filaments with markers of podosomes. Matrix metalloproteases are shuttled to the cell membrane to podosome-like structures in response to extracellular stimuli and mediate migration through cell tissue matrices<sup>17,27</sup>. Interestingly ADAMTS1, 4, and 5 have been previously been localized to podosome structures as well<sup>28</sup>. Based on our immunofluorescent staining and rodent models, it is possible that ADAMTS7 performs a similar function in vascular remodeling.

In conclusion, *ADAMTS7* is a genetic locus for CAD and MI in human, and our data are the first to show *in vivo* that *ADAMTS7* is pro-atherosclerotic and may promote progression and complications of the disease by modulating VSMC phenotype. Because *ADAMTS7* has narrow substrate specificity, it has promise as a potentially safe drug target. Our findings provide support for development of *ADAMTS7* inhibitors in prevention and treatment of human coronary atherosclerotic diseases.

## Supplementary Material

Refer to Web version on PubMed Central for supplementary material.

## Acknowledgements

We acknowledge Weili Yan for help with performing the wire injury experiments, and Andrea Stout for imaging assistance. The authors also thank the heart failure and transplant nurses, cardiothoracic surgeons, and operating room staff at the University of Pennsylvania and the Gift-of-Life donor program (Philadelphia, PA) for their assistance with heart tissue procurement.

**Funding Sources:** These studies were funded by NIH grant HL111694 (to M.P.R.) and Transatlantic Network of Excellence Grant 10CVD03 from the Fondation Leducq (to D.J.R.). M.P.R. is also supported by NIH grants DK090505, HL-113147, HL107643 and HL108636. R.C.B. is also supported by AHA Postdoctoral Fellowship 12040456.

## References

1. Go AS, Mozaffarian D, Roger VL, Benjamin EJ, Berry JD, Borden WB, Bravata DM, Dai S, Ford ES, Fox CS, Franco S, Fullerton HJ, Gillespie C, Hailpern SM, Heit JA, Howard VJ, Huffman MD, Kissela BM, Kittner SJ, Lackland DT, Lichtman JH, Lisabeth LD, Magid D, Marcus GM, Marelli A, Matchar DB, McGuire DK, Mohler ER, Moy CS, Mussolino ME, Nichol G, Paynter NP, Schreiner PJ, Sorlie PD, Stein J, Turan TN, Virani SS, Wong ND, Woo D, Turner MB. on behalf of the American Heart Association Statistics Committee and Stroke Statistics Subcommittee. Executive Summary: Heart Disease and Stroke Statistics--2013 Update: A Report From the American Heart Association. *Circulation*. 2013; 127:143–152. [PubMed: 23283859]
2. Reilly MP, Li M, He J, Ferguson JF, Stylianou IM, Mehta NN, Burnett MS, Devaney JM, Knouff CW, Thompson JR, Horne BD, Stewart AFR, Assimes TL, Wild PS, Allayee H, Nitschke PL, Patel RS, Myocardial Infarction Genetics Consortium, Wellcome Trust Case Control Consortium, Martinelli N, Girelli D, Quyyumi AA, Anderson JL, Erdmann J, Hall AS, Schunkert H, Quertermous T, Blankenberg S, Hazen SL, Roberts R, Kathiresan S, Samani NJ, Epstein SE, Rader DJ, Qasim AN, DerOhannessian SL, Qu L, Cappola TP, Chen Z, Matthai W, Hakonarson HH, Wilensky R, Kent KM, Lindsay JM, Pichard AD, Satler L, Waksman R. Identification of

ADAMTS7 as a novel locus for coronary atherosclerosis and association of ABO with myocardial infarction in the presence of coronary atherosclerosis: two genome-wide association studies. *Lancet*. 2011; 377:383–392. [PubMed: 21239051]

3. Schunkert H, König IR, Kathiresan S, Reilly MP, Assimes TL, Holm H, Preuss M, Stewart AFR, Barbalic M, Gieger C, Absher D, Aherrahrou Z, Allayee H, Altshuler D, Anand SS, Andersen K, Anderson JL, Ardissino D, Ball SG, Balmforth AJ, Barnes TA, Becker DM, Becker LC, Berger K, Bis JC, Boekholdt SM, Boerwinkle E, Braund PS, Brown MJ, Burnett MS, Buyschaert I, Cardiogenics, Carlquist JF, Chen L, Cichon S, Codd V, Davies RW, Dedoussis G, Dehghan A, Demissie S, Devaney JM, Diemert P, Do R, Doering A, Eifert S, Mokhtari NEE, Ellis SG, Elosua R, Engert JC, Epstein SE, de Faire U, Fischer M, Folsom AR, Freyer J, Gigante B, Girelli D, Gretarsdottir S, Gudnason V, Gulcher JR, Halperin E, Hammond N, Hazen SL, Hofman A, Horne BD, Illig T, Iribarren C, Jones GT, Jukema JW, Kaiser MA, Kaplan LM, Kastelein JJP, Khaw K-T, Knowles JW, Kolovou G, Kong A, Laaksonen R, Lambrechts D, Leander K, Lettre G, Li M, Lieb W, Loley C, Lotery AJ, Mannucci PM, Maouche S, Martinelli N, McKeown PP, Meisinger C, Meitinger T, Melander O, Merlini PA, Mooser V, Morgan T, Mühleisen TW, Muhlestein JB, Münzel T, Musunuru K, Nahrstaedt J, Nelson CP, Nöthen MM, Olivieri O, Patel RS, Patterson CC, Peters A, Peyvandi F, Qu L, Quyyumi AA, Rader DJ, Rallidis LS, Rice C, Rosendaal FR, Rubin D, Salomaa V, Sampietro ML, Sandhu MS, Schadt E, Schäfer A, Schillert A, Schreiber S, Schrezenmeier J, Schwartz SM, Siscovick DS, Sivananthan M, Sivapalaratnam S, Smith A, Smith TB, Snoep JD, Soranzo N, Spertus JA, Stark K, Stirrups K, Stoll M, Tang WH, Tennstedt S, Thorgeirsson G, Thorleifsson G, Tomaszewski M, Uitterlinden AG, van Rij AM, Voight BF, Wareham NJ, Wells GA, Wichmann HE, Wild PS, Willenborg C, Wittmann JC, Wright BJ, Ye S, Zeller T, Ziegler A, Cambian F, Goodall AH, Cupples LA, Quertermous T, März W, Hengstenberg C, Blankenberg S, Ouwehand WH, Hall AS, Deloukas P, Thompson JR, Stefansson K, Roberts R, Thorsteinsdottir U, O'Donnell CJ, McPherson R, Erdmann J, CARDIOGRAM Consortium. Samani NJ. Large-scale association analysis identifies 13 new susceptibility loci for coronary artery disease. *Nat Genet*. 2011; 43:333–338. [PubMed: 21378990]
4. Coronary Artery Disease (C4D) Genetics Consortium. A genome-wide association study in Europeans and South Asians identifies five new loci for coronary artery disease. *Nat Genet*. 2011; 43:339–344. [PubMed: 21378988]
5. CARDIOGRAMplusC4D Consortium; Deloukas P, Kanoni S, Willenborg C, Farrall M, Assimes TL, Thompson JR, Ingelsson E, Saleheen D, Erdmann J, Goldstein BA, Stirrups K, König IR, Cazier J-B, Johansson Å, Hall AS, Lee J-Y, Willer CJ, Chambers JC, Esko T, Folkersen L, Goel A, Grundberg E, Havulinna AS, Ho WK, Hopewell JC, Eriksson N, Kleber ME, Kristiansson K, Lundmark P, Lytikäinen L-P, Rafelt S, Shungin D, Strawbridge RJ, Thorleifsson G, Tikkanen E, Van Zuydam N, Voight BF, Waite LL, Zhang W, Ziegler A, Absher D, Altshuler D, Balmforth AJ, Barroso I, Braund PS, Burgdorf C, Claudi-Boehm S, Cox D, Dimitriou M, Do R, DIAGRAM Consortium, CARDIOGENICS Consortium; Doney ASF, Mokhtari El N, Eriksson P, Fischer K, Fontanillas P, Franco-Cereceda A, Gigante B, Groop L, Gustafsson S, Hager J, Hallmans G, Han B-G, Hunt SE, Kang HM, Illig T, Kessler T, Knowles JW, Kolovou G, Kuusisto J, Langenberg C, Langford C, Leander K, Lokki M-L, Lundmark A, McCarthy MI, Meisinger C, Melander O, Mihailov E, Maouche S, Morris AD, Müller-Nurasyid M, MuTHER Consortium; Nikus K, Peden JF, Rayner NW, Rasheed A, Rosinger S, Rubin D, Rumpf MP, Schäfer A, Sivananthan M, Song C, Stewart AFR, Tan S-T, Thorgeirsson G, van der Schoot CE, Wagner PJ, Wellcome Trust Case Control Consortium. Wells GA, Wild PS, Yang TP, Amouyel P, Arveiler D, Basart H, Boehnke M, Boerwinkle E, Brambilla P, Cambien F, Cupples AL, de Faire U, Dehghan A, Diemert P, Epstein SE, Evans A, Ferrario MM, Ferrières J, Gauguier D, Go AS, Goodall AH, Gudnason V, Hazen SL, Holm H, Iribarren C, Jang Y, Kähönen M, Kee F, Kim HS, Klopp N, Koenig W, Kratzer W, Kuulasmaa K, Laakso M, Laaksonen R, Lee JY, Lind L, Ouwehand WH, Parish S, Park JE, Pedersen NL, Peters A, Quertermous T, Rader DJ, Salomaa V, Schadt E, Shah SH, Sinisalo J, Stark K, Stefansson K, Trégouët DA, Virtamo J, Wallentin L, Wareham N, Zimmermann ME, Nieminen MS, Hengstenberg C, Sandhu MS, Pastinen T, Syvänen AC, Hovingh GK, Dedoussis G, Franks PW, Lehtimäki T, Metspalu A, Zalloua PA, Siegbahn A, Schreiber S, Ripatti S, Blankenberg SS, Perola M, Clarke R, Boehm BO, O'Donnell C, Reilly MP, März W, Collins R, Kathiresan S, Hamsten A, Kooner JS, Thorsteinsdottir U, Danesh J, Palmer CN, Roberts R, Watkins H, Schunkert H, Samani NJ. Large-scale association analysis identifies new risk loci for coronary artery disease. *Nat Genet*. 2013; 45:25–33. [PubMed: 23202125]

6. Hurskainen TL, Hirohata S, Seldin MF, Apte SS. ADAM-TS5, ADAM-TS6, and ADAM-TS7, novel members of a new family of zinc metalloproteases. General features and genomic distribution of the ADAM-TS family. *J Biol Chem.* 1999; 274:25555–25563. [PubMed: 10464288]
7. Somerville RPT, Longpré J-M, Apel ED, Lewis RM, Wang LW, Sanes JR, Leduc R, Apte SS. ADAMTS7B, the full-length product of the ADAMTS7 gene, is a chondroitin sulfate proteoglycan containing a mucin domain. *J Biol Chem.* 2004; 279:35159–35175. [PubMed: 15192113]
8. Porter S, Clark IM, Kevorkian L, Edwards DR. The ADAMTS metalloproteinases. *Biochem J.* 2005; 386:15–27. [PubMed: 15554875]
9. Gao W, Zhu J, Westfield LA, Tuley EA, Anderson PJ, Sadler JE. Rearranging Exosites in Noncatalytic Domains Can Redirect the Substrate Specificity of ADAMTS Proteases. *J Biol Chem.* 2012; 287:26944–26952. [PubMed: 22707719]
10. Liu C-J, Kong W, Ilalov K, Yu S, Xu K, Prazak L, Fajardo M, Sehgal B, Di Cesare PE. ADAMTS-7: a metalloproteinase that directly binds to and degrades cartilage oligomeric matrix protein. *FASEB J.* 2006; 20:988–990. [PubMed: 16585064]
11. Bai X-H, Wang D-W, Kong L, Zhang Y, Luan Y, Kobayashi T, Kronenberg HM, Yu X-P, Liu C-J. ADAMTS-7, a direct target of PTHrP, adversely regulates endochondral bone growth by associating with and inactivating GEP growth factor. *Mol Cell Biol.* 2009; 29:4201–4219. [PubMed: 19487464]
12. Riessen R, Fenchel M, Chen H, Axel DI, Karsch KR, Lawler J. Cartilage oligomeric matrix protein (thrombospondin-5) is expressed by human vascular smooth muscle cells. *Arterioscler Thromb Vasc Biol.* 2001; 21:47–54. [PubMed: 11145932]
13. Wang L, Zheng J, Bai X, Liu B, Liu C-J, Xu Q, Zhu Y, Wang N, Kong W, Wang X. ADAMTS-7 mediates vascular smooth muscle cell migration and neointima formation in balloon-injured rat arteries. *Circ Res.* 2009; 104:688–698. [PubMed: 19168437]
14. Tangirala RK, Tsukamoto K, Chun SH, Usher D, Pure E, Rader DJ. Regression of Atherosclerosis Induced by Liver-Directed Gene Transfer of Apolipoprotein A-I in Mice. *Circulation.* 1999; 100:1816–1822. [PubMed: 10534470]
15. Wang L, Wang X, Kong W. ADAMTS-7, a novel proteolytic culprit in vascular remodeling. *Sheng Li Xue Bao.* 2010; 62:285–294. [PubMed: 20717629]
16. Owens GK. Molecular Regulation of Vascular Smooth Muscle Cell Differentiation in Development and Disease. *Physiol Rev.* 2004; 84:767–801. [PubMed: 15269336]
17. Murphy DA, Courtneidge SA. The ‘ins’ and ‘outs’ of podosomes and invadopodia: characteristics, formation and function. *Nat Genet.* 2011; 12:413–426.
18. Moake JL. Thrombotic microangiopathies. *N Engl J Med.* 2002; 347:589–600. [PubMed: 12192020]
19. Dagoneau N, Benoist-Lassel C, Huber C, Faivre L, Mégarbané A, Alswaid A, Dollfus H, Alembik Y, Munnich A, Legeai-Mallet L, Cormier-Daire V. ADAMTS10 Mutations in Autosomal Recessive Weill-Marchesani Syndrome. *Am J Hum Genet.* 2004; 75:801–806. [PubMed: 15368195]
20. Salter RC, Ashlin TG, Kwan APL, Ramji DP. ADAMTS proteases: key roles in atherosclerosis? *J Mol Med.* 2010; 88:1203–1211. [PubMed: 20652528]
21. Wang L, Zheng J, Du Y, Huang Y, Li J, Liu B, Liu C-J, Zhu Y, Gao Y, Xu Q, Kong W, Wang X. Cartilage Oligomeric Matrix Protein Maintains the Contractile Phenotype of Vascular Smooth Muscle Cells by Interacting With  $\alpha 1$  Integrin. *Circ Res.* 2010; 106:514–525. [PubMed: 20019333]
22. Ohta H, Wada H, Niwa T, Kirii H, Iwamoto N, Fujii H, Saito K, Sekikawa K, Seishima M. Disruption of tumor necrosis factor- $\alpha$  gene diminishes the development of atherosclerosis in ApoE-deficient mice. *Atherosclerosis.* 2005; 180:11–17. [PubMed: 15823270]
23. Inflammatory markers and cardiovascular disease (The Health, Aging and Body Composition [Health ABC] Study). *Am J Cardiol.* 2003; 92:522–528. [PubMed: 12943870]
24. Jovinge S, Hultgardh-Nilsson A, Regnstrom J, Nilsson J. Tumor necrosis factor-alpha activates smooth muscle cell migration in culture and is expressed in the balloon-injured rat aorta. *Arterioscler Thromb Vasc Biol.* 1997; 17:490–497. [PubMed: 9102167]
25. Grundberg E, Small KS, Hedman ÅK, Nica AC, Buil A, Keildson S, Bell JT, Yang T-P, Meduri E, Barrett A, Nisbett J, Sekowska M, Wilk A, Shin S-Y, Glass D, Travers M, Min JL, Ring S, Ho K,

- Thorleifsson G, Kong A, Thorsteindottir U, Ainali C, Dimas AS, Hassanali N, Ingle C, Knowles D, Krestyaninova M, Lowe CE, Di Meglio P, Montgomery SB, Parts L, Potter S, Surdulescu G, Tsaprouni L, Tsoka S, Bataille V, Durbin R, Nestle FO, O'Rahilly S, Soranzo N, Lindgren CM, Zondervan KT, Ahmadi KR, Schadt EE, Stefansson K, Smith GD, McCarthy MI, Deloukas P, Dermitzakis ET, Spector TD. Mapping cis- and trans-regulatory effects across multiple tissues in twins. *Nat Genet.* 2012; 44:1084–1089. [PubMed: 22941192]
26. Pu X, Xiao Q, Kiechl S, Chan K, Ng FL, Gor S, Poston RN, Fang C, Patel A, Senver EC, Shaw-Hawkins S, Willeit J, Liu C, Zhu J, Tucker AT, Xu Q, Caulfield MJ, Ye S. ADAMTS7 Cleavage and Vascular Smooth Muscle Cell Migration Is Affected by a Coronary-Artery- Disease-Associated Variant. *Am J Hum Genet.* 2013; 92:366–74. doi: 10.1016/j.ajhg.2013.01.012. Epub 2013 Feb 14. [PubMed: 23415669]
27. Zucker S, Hymowitz M, Conner CE, DiYanni EA, Cao J. Rapid Trafficking of Membrane Type 1-Matrix Metalloproteinase to the Cell Surface Regulates Progelatinase A Activation. *Lab Invest.* 2002; 82:1673–1684. [PubMed: 12480917]
28. Keller KE, Bradley JM, Acott TS. Differential Effects of ADAMTS-1, -4, and -5 in the Trabecular Meshwork. *Invest Ophthalmol Vis Sci.* 2009; 50:5769–5777. [PubMed: 19553617]

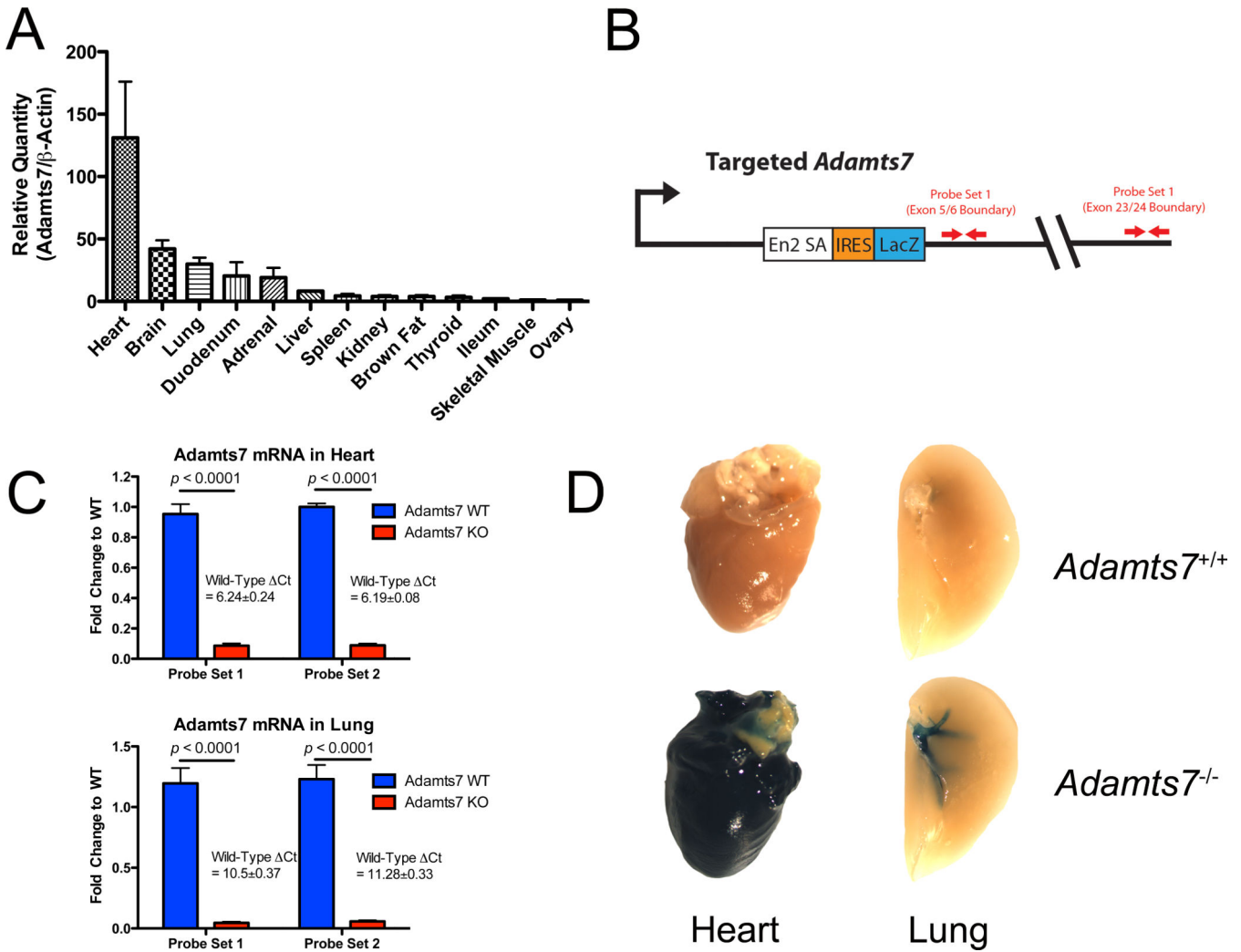


**Figure 1.** Characterization of *Adamts7*<sup>-/-</sup> Mice. A) Assessment of *Adamts7* expression in multiple tissues from the mouse (N=3). Data is shown as relative quantity (to  $\beta$ -actin) and represented as fold-change over the lowest expressing tissue. B) Schematic of the targeting strategy used in creation of the *Adamts7*<sup>-/-</sup> mouse, and the location of TaqMan probesets used in confirmation of KO of the gene expression. C) TaqMan realtime qPCR measurements of expression of *Adamts7* in heart and lung tissue from WT and KO mice (N=6/group) showing near complete loss of expression of *Adamts7*. Data from the two probe-sets identified in Figure 1B are shown. D) Overnight X-gal staining of select tissues from WT and KO animals confirms the realtime qPCR data and further illustrates expression patterns of *Adamts7* in these tissues.



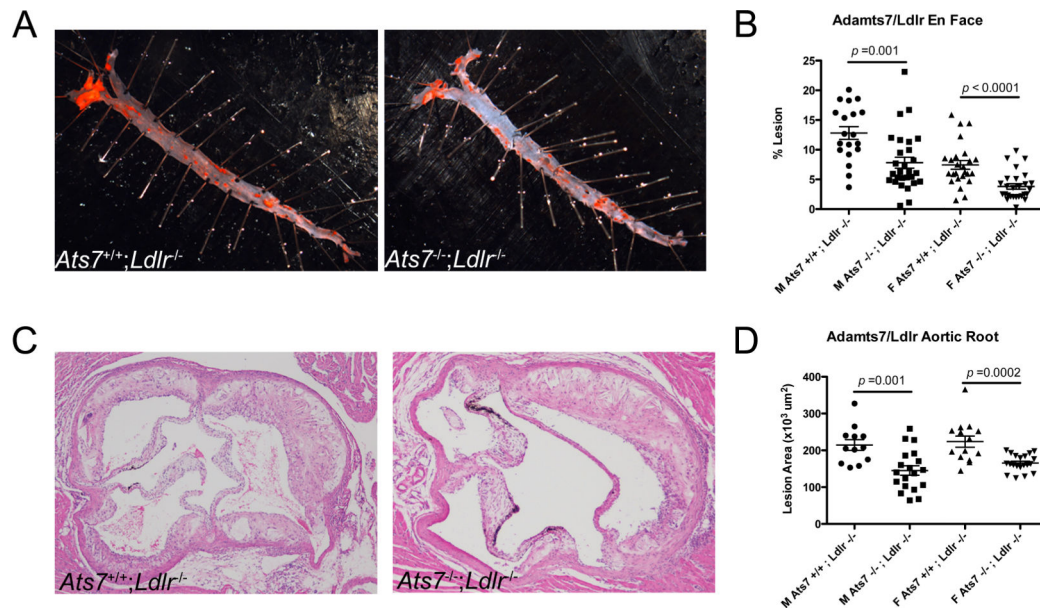


**Figure 2.**

*Adamts7* deficiency reduces atherosclerosis in the *Ldlr* KO hyperlipidemic mouse model. A) Representative oil-red O stained aortas from male *Adamts7*<sup>+/+</sup>/*Ldlr*<sup>-/-</sup> and *Adamts7*<sup>-/-</sup>/*Ldlr*<sup>-/-</sup> mice after 16-weeks of western diet feeding. B) Quantification of atherosclerosis in the aortas of these mice, both male (N=21, 31) and female (N=28, 34). Lesion area is represented as percent area of the entire aorta. C) Representative H/E stained aortic roots from male *Adamts7*<sup>+/+</sup>/*Ldlr*<sup>-/-</sup> and *Adamts7*<sup>-/-</sup>/*Ldlr*<sup>-/-</sup> mice. D) Quantification of aortic root lesion area between the two animal groups in both sexes. Lesion area was calculated in 5 serial sections through the aortic root, and an average value was obtained for each mouse.

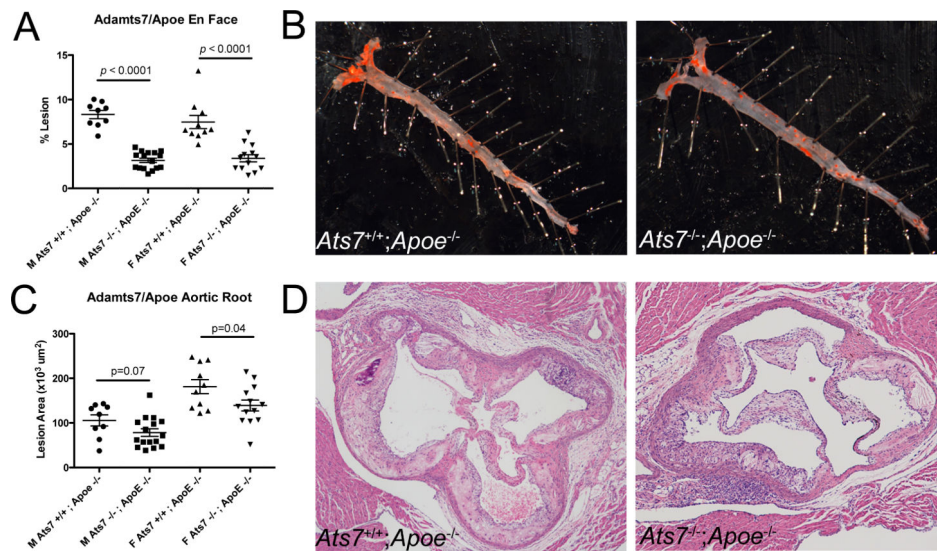


**Figure 3.**

*Adamts7* deficiency also reduces atherosclerotic burden in the *Apoe* KO hyperlipidemic mouse model on western diet. A) Quantification of area staining positive for oil-red O for both *Adamts7*<sup>+/+</sup>; *Apoe*<sup>-/-</sup> and *Adamts7*<sup>-/-</sup>; *Apoe*<sup>-/-</sup> control littermates from both sexes (Males N=9, 16; Females N=10, 13) after being fed western diet for 10 weeks. B) Representative oil-red O stained aortas from male *Adamts7*<sup>+/+</sup>; *Apoe*<sup>-/-</sup> and *Adamts7*<sup>-/-</sup>; *Apoe*<sup>-/-</sup> animals. C) Average lesion area across 5 serial sections from the aortic roots of *Adamts7*<sup>+/+</sup>; *Apoe*<sup>-/-</sup> and *Adamts7*<sup>-/-</sup>; *Apoe*<sup>-/-</sup> animals. D) Representative H/E stained sections from male KO and dKO animals used in the studies.

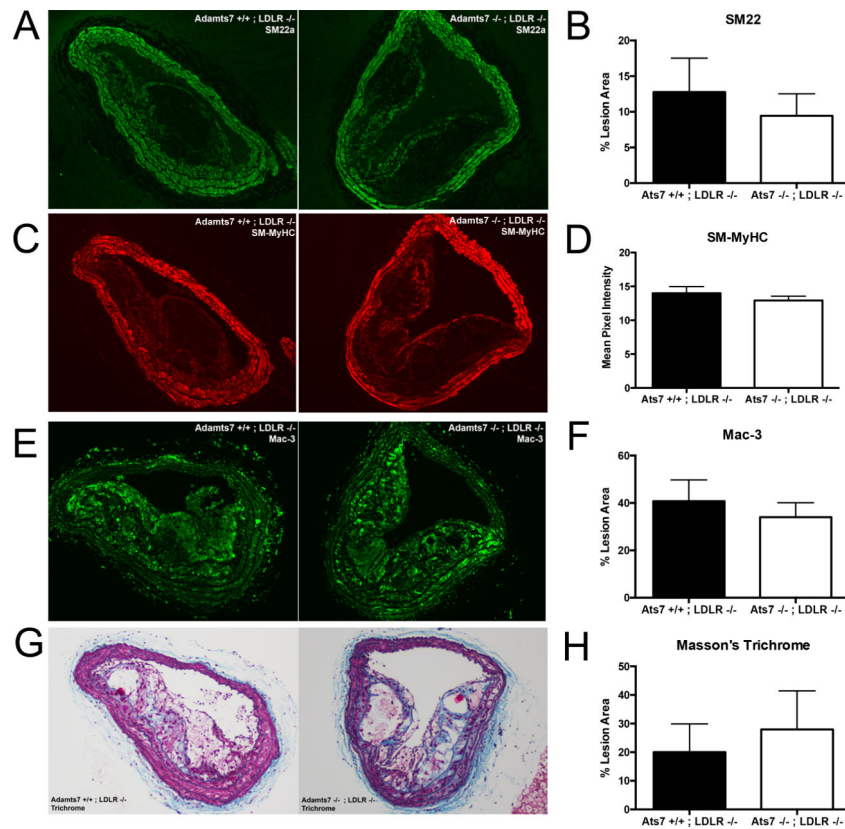


**Figure 4.** Smooth muscle cell, macrophage, and collagen staining of brachiocephalic artery (BCA) lesions from *Adamts7*<sup>-/-</sup>;*Ldlr*<sup>-/-</sup> animals compared to controls. Representative IHC staining of SM22 (A), SM-MyHC (C), Mac-3 (E), and Masson's Trichrome (G) from the BCAs of *Adamts7*<sup>-/-</sup>;*Ldlr*<sup>-/-</sup> animals and control littermates (N=9/group) are shown. Quantification of the positive signal inside the lesion (B, D, F) or the blue staining in the trichrome (H) is shown to the right of the images and presented as percent of lesion area or mean pixel intensity.

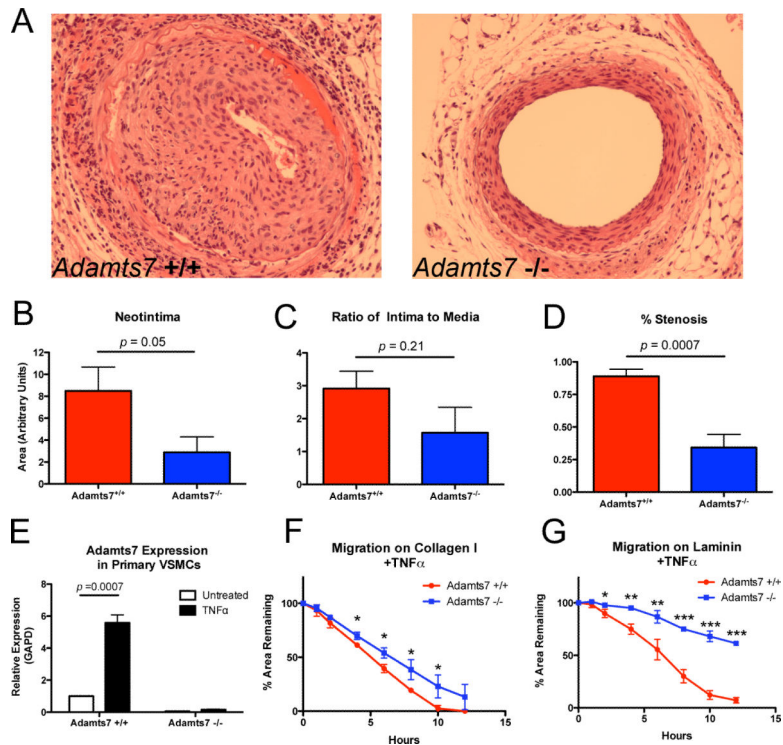


**Figure 5.**

Neointima formation following femoral artery wire injury is attenuated by ablation of mouse *Adamts7*. (A) Wire injury was performed on femoral arteries of *Adamts7*<sup>-/-</sup> and WT animals (N=5 and 4, respectively), vessels were harvested at 28 days and neointima was assessed by H/E staining. Representative sections from WT and KO femoral arteries are shown. There was reduced (B) neointima (64%), (C) intima-to-media ratio (47%) and (D) percent stenosis (61%) in *Adamts7*<sup>-/-</sup> compared to WT. (E) *Adamts7* expression measured by TaqMan real-time qPCR in primary VSMCs from *Adamts7* WT or KO mice after treatment with 25ng/ml TNF $\alpha$  for 24-hours (N=3). (F,G) Migration of TNF $\alpha$ -stimulated *Adamts7* KO primary VSMCs on collagen or laminin coated plates (N=3) is reduced compared to WT cells.



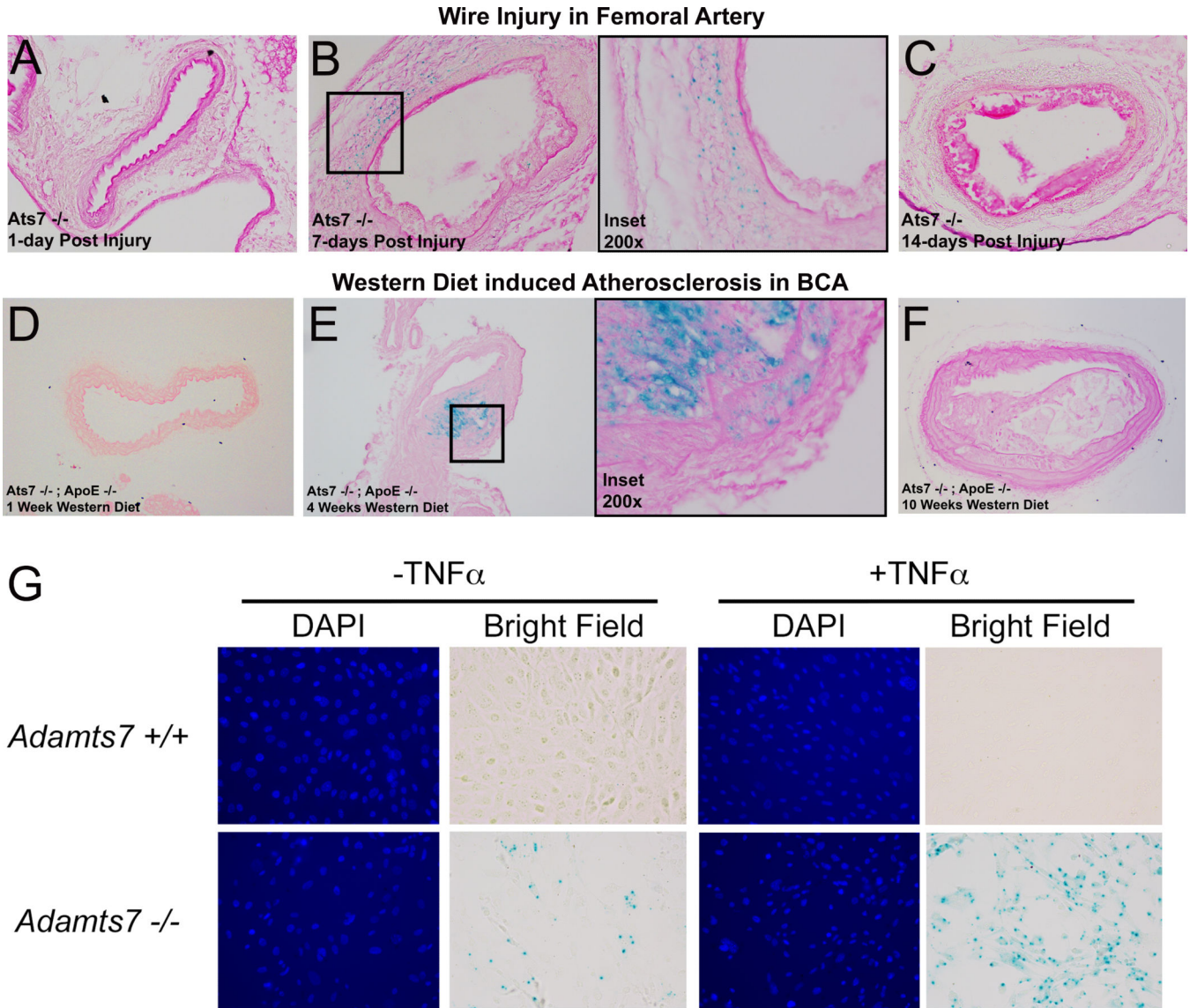


**Figure 6.** *Adamts7* vascular expression is transiently induced in response to mechanical and hyperlipidemic stress in mouse models. (A-C) Femoral arteries were X-gal stained overnight at the indicated timepoints (N=4/timepoint) following endothelial denudation by wire injury. Representative sections from the resultant stained injured vessels are shown revealing positive X-gal staining in the media and adventitia of vessels 7 days post-injury. Panel B includes increased magnification of the boxed region from the 7-day injury. (D-F) X-gal staining of atherosclerotic BCA lesions from *Adamts7*<sup>-/-</sup>;*ApoE*<sup>-/-</sup> mice fed western diet for 1, 4, and 10 weeks (N=3/timepoint). Panel E includes higher magnification of the boxed region from the 4-week lesion. (G) X-gal staining in primary VSMCs with and without 24-hour treatment with 25ng/ml TNF $\alpha$ .

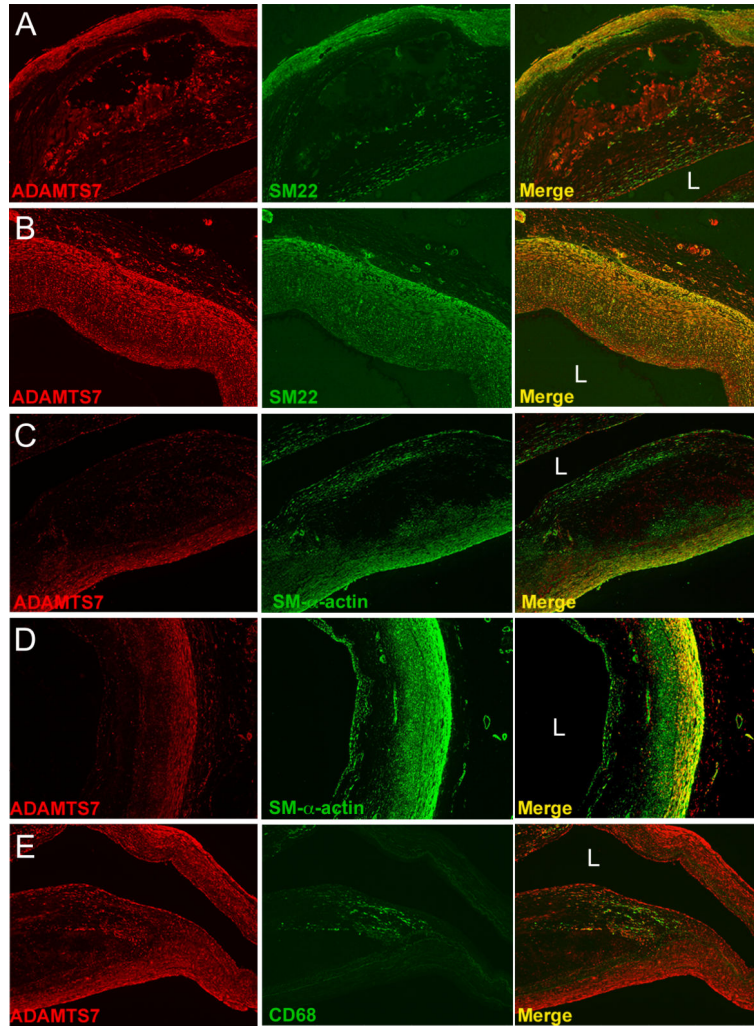


**Figure 7.** ADAMTS7 colocalizes with VSMC markers in human atherosclerotic coronary artery sections. (A,B) Staining of human coronary artery lesions with antibodies directed towards ADAMTS7 and SM22, with merge of the two stains shown in the far right panels. (C, D) Staining of similar lesions shown in A and B for ADAMTS7 and SM- $\alpha$ -actin, with merge shown in far right columns. (E) Staining of the shoulder region of a human coronary artery lesion with antibodies to ADAMTS7 and CD68, with merge to the far right showing little overlap between the two stains. “L” denotes location of the lumen. Staining was performed in 12 different diseased human coronary artery samples, and representative images are shown.



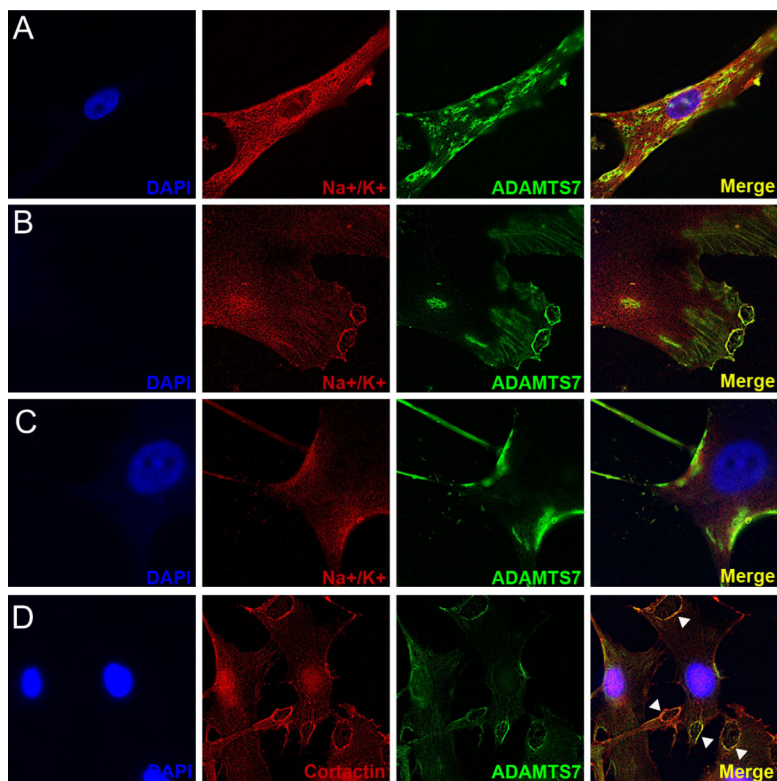


**Figure 8.** ADAMTS7 localizes to the leading edge and podosome-like structures in primary human aortic smooth muscle cells (hAoSMCs). (A-C) immunofluorescent staining for ADAMTS7 and the cell surface marker Na<sup>+</sup>/K<sup>+</sup> Ion Channel in primary human aortic SMCs. Each row is imaging of a different cell in the same experiment. (D) Co-staining for ADAMTS7 and cortactin, a marker of podosomes, in primary hAoSMCs. Arrowheads identify regions of strong overlap in focal adhesion-like structures.